Atomic alchemy: Weak decays of muonic and pionic atoms into other atoms

C. Greub and D. Wyler
Institut für Theoretische Physik, Universität Zürich, Zürich, Switzerland

S. J. Brodsky and C. T. Munger
Stanford Linear Accelerator Center, Stanford University, Stanford, California 94309
(Received 9 May 1994)

The rates of weak transitions between electromagnetic bound states, for example, $(\pi^+e^-) \to (\mu^+e^-)\nu_\mu$, and the exclusive weak decay of a muonic atom into an electronic atom, $(Z\mu^-) \to (Ze^-)\nu_\mu\bar{\nu}_e$, are calculated. For $Z = 80$, relativistic effects are shown to increase the latter rate by a factor of 50 compared to the results of a nonrelativistic calculation. It is argued that the conditions for producing the muonic decay in neon gas ($Z = 10$), where the branching ratio for the decay per captured muon is 1.7×10^{-9}, can be realized using cyclotron traps, though the prospect for a practical experiment seems remote. In lead the same ratio would be approximately $\sim 1 \times 10^{-6}$. In addition to providing detailed information on the high momentum tail of the wave functions in atomic physics, these decays of QED bound states provide a simple toy model for investigating kinematically analogous situations in exclusive heavy hadronic decays in quantum chromodynamics, such as $B \to K^*\gamma$ or $B \to \pi e\nu$.

PACS number(s): 36.10.Dr, 11.10.St, 13.20.He, 13.35.−r

I. INTRODUCTION

The calculation of the rate of a weak decay of a heavy meson into an exclusive channel, such as $B \to \gamma K^*$ as $B \to De\nu$, poses an important and challenging problem in nonperturbative quantum chromodynamics because all the complexities of strong interactions enter. In this paper we study the simpler non-Abelian analogues of these processes in atomic physics, the weak decays of one electromagnetic bound state into another. In QED the calculation can be done exactly for bound states at rest and their motion can be systematically taken into account. In both the non-Abelian and the Abelian case, one is sensitive to the high momentum tail of the wave functions, and, in fact, there are important relations between the two theories. It was shown that in high momentum transfer reactions the factorization theorems are the same once one adjusts for the differing β function [1]; additionally, the heavy quark symmetries are the same [2].

Thus, we consider transitions of the form

$$(\pi^+e^-) \to (\mu^+e^-)\nu_\mu \ , \qquad (Z\mu^-) \to (Ze^-)\nu_\mu\bar{\nu}_e \ . \tag{1}$$

The latter process is particularly interesting because large values of the nucleus charge Z make the effective electromagnetic coupling constant strong, thus suggesting an analogy to the QCD coupling constant. In addition, the process may be experimentally accessible, albeit with great difficulty, using cyclotron traps.

Because the atom remains in a bound state, but the atomic or nuclear species is changed, we refer to such processes as "atomic alchemy." Other examples of atomic alchemy are the decay of muonium to positronium, $(\mu^+e^-) \to (e^+e^-)\bar{\nu}_\mu\nu_e$, and the decays of mesonic and hadronic atoms such as $(\pi^-Z) \to (\mu^-Z)\bar{\nu}_\mu$ and $(\Sigma^-Z) \to (\bar{p}Z)\pi^0$. However, observation of the muonic transition just mentioned is impractical because of its tiny branching ratio with respect to the decay of the muon into a free electron, and observation of the others is impractical because of the high rate at which hadrons are absorbed by the nucleus.

Another interesting class of "induced atomic alchemy" occurs when a nucleus is forced to change its state because of external scattering, while an atomic electron remains bound. The scattering may be due to neutron-induced fission, nuclear Compton scattering, or photodisintegration; the latter is particularly interesting for deuterium, $\gamma(d^+e^-) \to (p^+e^-)n$. One can also study atomic alchemy when a nucleus changes its state by an internal process, such as β decay. Similarly, one might consider the observed reactions $K \to (\pi\mu)\nu$ and $(\mu dt) \to (\mu\alpha)n$.

In this paper, we concentrate on the exclusive transition, $B_1 \to B_2 + X$, where both B_1 and B_2 are bound states consisting of particles $(b_1 s)$ and $(b_2 s)$, respectively, and the transition proceeds by a weak decay $b_1 \to b_2 + X$. To justify the calculations of the branching ratios given below, we require that the $1S$ state in B_2 will be empty to receive the particle b_2, so that the Pauli principle does not block the largest branch for the decay. We also require that the rate at which the spectator absorbs the particle b_1, instead of allowing it to decay, is negligible. Both requirements are easily met in the decay $(\pi^+e^-) \to (\mu^+e^-)\nu_\mu$; however, in the decay of bound muons, $(Z\mu^-) \to (Ze^-)\nu_\mu\bar{\nu}_e$, they can be met in practice only with great difficulty. These problems we address in Sec. IV.

The basic features of atomic alchemy can be easily understood using nonrelativistic mechanics; the analysis is similar to that for nuclear collisions involving capture of

atomic electrons, as discussed, for example, by Migdal [3]. We review the major points before plunging into the full relativistic calculation. Because the weak decay occurs over a time short compared to the period of an orbit, we can use the "sudden approximation." The probability amplitude for the atomic transition then factors into the free matrix element of the weakly decaying (moving) particle times a form factor $F(\vec{q}^2)$. This form factor is just the overlap of the wave functions of the initial and final states, which we write as ψ_1 and ψ_2. In the rest frame of the initial state, $F(\vec{q}^2)$ is

$$F(\vec{q}^2) = \int \frac{d^3k_1}{(2\pi)^3}\psi_1(\vec{k}_1)\psi_2^*(\vec{k}_2 = m_{\mathrm{red},2}\vec{v}_{\mathrm{rel},2}) \ . \quad (2)$$

Here $\vec{k}_1$ is the momentum of b_1 (see Fig. 1), and $m_{\mathrm{red},2}$ and $\vec{v}_{\mathrm{rel},2}$ are the reduced mass and the relative velocity of the final state particles b_2 and s. The velocity $\vec{v}_{\mathrm{rel},2}$ is a function of $\vec{q}$, the momentum transfer carried by X, which by conservation of momentum is equal to the recoil momentum of B_2. We have

$$\vec{v}_{\mathrm{rel},2} = \frac{\vec{k}_1 - \vec{q}}{m_{b_2}} + \frac{\vec{k}_1}{m_s} = \frac{\vec{k}_1}{m_{\mathrm{red},2}} - \frac{\vec{q}}{m_{b_2}} \ . \quad (3)$$

In the decay $(Z\mu^-) \to (Ze^-)\nu_\mu\bar{\nu}_e$, the argument $\vec{k}_2$ of the wave function ψ_2^* is approximately $\vec{k}_2 \approx \vec{k}_1 - \vec{q}$. In momentum space the muon wave function does not vary much over the domain where the electron wave function differs appreciably from zero. The integral in Eq. (2) can therefore be approximated by

$$F(\vec{q}^2) = \psi_1(\vec{q})\psi_2^*(\vec{r} = 0) \ . \quad (4)$$

For small Z the momenta of both the muon and the electron are nonrelativistic and the effects of the finite nucleus size are small; we therefore can use for ψ_1 and ψ_2 the Schrödinger wave functions for a point nucleus. For the $1S$ states

$$\psi_i(\vec{k}) = \frac{8\sqrt{\pi}a_i^{3/2}}{[1 + a_i^2\vec{k}^2]^2}, \quad a_i = \frac{1}{m_{\mathrm{red},i}Z\alpha} \quad (i = 1,2) \ , \quad (5)$$

where a_i denote the Bohr radii of the atoms. Because $\psi_i(\vec{r} = 0) = [\sqrt{\pi}a_i^{(3/2)}]^{-1}$, Eq. (4) becomes

$$F(\vec{q}^2) = 8\left(\frac{m_e}{m_\mu}\right)^{3/2}\left[\frac{1}{1 + \vec{q}^2/(Z\alpha m_\mu)^2}\right]^2 \ . \quad (6)$$

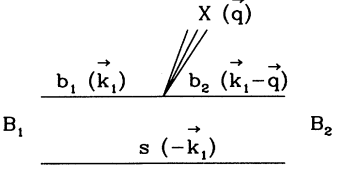

FIG. 1. General diagram for a weak alchemy transition $B_1 \to B_2 + X$ as discussed in the text. The momenta of the particles are indicated in parentheses.

The physics of capture into a hydrogenic nS state is controlled by the ratio of the change in nuclear velocity to the atomic velocity $Z\alpha/n$. Equation (6) suggests that the highest rates for the transition of muonic to electronic atoms will be found for heavy nuclei with $(Z\alpha m_\mu)^2 \geq \vec{q}^2$. For these atoms, however, Eq. (6) provides only a very rough estimate for the form factor because relativistic effects [mainly affecting the wave function of the (Ze^-) atom] become crucial and greatly enhance the transition rate.

In the case of the transition $(\pi^+e^-) \to (\mu^+e^-)\nu_\mu$, the monoenergetic weak decay changes the species and velocity of the heavy particle serving as a nucleus. Since the momentum transfer from the pion to the muon is much larger than either Bohr momentum, the integrand in the form factor in Eq. (2) is dominated by those values of k_1 for which either k_1 or k_2 matches a Bohr momentum. Both contributions turn out to be equally important, and using for the $1S$ states the Schrödinger wave functions for a Coulomb potential, we obtain for the form factor

$$F(\vec{q}^2) \simeq 2\psi_1(\vec{r} = 0)\psi_2^*(m_{\mathrm{red},2}\vec{v}_{\mathrm{rel},2}) \simeq 16\left(\frac{\alpha}{v_{\mathrm{rel},2}}\right)^4 \ . \quad (7)$$

Here $v_{\mathrm{rel},2} = (m_\pi^2 - m_\mu^2)/(2m_\pi m_\mu) = 0.28$, which is small enough that our nonrelativistic treatment is justified. The probability for capture of the electron from the muonic decay is unfortunately very small:

$$P = [F(\vec{q}^2)]^2 \simeq 256\alpha^8/v_{\mathrm{rel},2}^8 \sim 5 \times 10^{-11} \ . \quad (8)$$

II. RELATIVISTIC ANALYSIS OF ATOMIC TRANSITIONS

We now turn to a more detailed analysis which allows us to treat decays such as $(Z\mu^-) \to (Ze^-)\nu_\mu\bar{\nu}_e$, where for large Z the velocities of the bound constituents are relativistic. In principle, the analysis requires a fully covariant description, such as the Bethe-Salpeter equation or the light-cone Fock state expansion. In Ref. [4] such a covariant description was given, but at the expense of a somewhat artificial momentum-dependent mass for the decaying constituent. While that description works well when the decaying constituent is much heavier than the spectator, it fails when the spectator is the heavier particle, because the high momenta of the constituents, which prove crucial, are cut off [see Eq. (2.1) of Ref. [4]]. Here we use a noncovariant description that is adequate for the cases of interest, where the spectators in the initial and final bound states have small relative velocity, but where the velocities of the particles bound to the spectators can be relativistic. This description is particularly appropriate for the transition $(\mu^-Z) \to (e^-Z) + \nu_\mu\bar{\nu}_e$ because the mass of a nucleus is much greater than m_μ.

We begin with a relativistic treatment of the simple, monoenergetic, two-body atomic transition $(\pi^+e^-) \to (\mu^+e^-) + \nu_\mu$. The relative velocity of the (πe) and (μe) systems is only $v_{\mathrm{rel}} = 0.28$, so one can simplify the kine-

matics by assuming them to be at relative rest. We consider only S-wave bound states, so the spin of the bound state B_1 is just the spin of the electron, and the final bound state B_2 is either a pseudoscalar or a vector particle with the corresponding well-known spin combinations of the constituents. For example, the initial state B_1 with spin projection R is represented in its rest frame as

$$|B_1,\vec{p}_B=0,R\rangle=\sqrt{2m_{B_1}}\int\frac{d^3k_1}{\sqrt{4k_1^0k_3^0}(2\pi)^3}\times\psi_1(\vec{k}_1)a_R^+(\vec{k}_1)b^+(\vec{k}_3)|0\rangle\ , \tag{9}$$

where $\vec{k}_3=-\vec{k}_1$, and $k_i^0=(\vec{k}_i^2+m_i^2)^{1/2}$ for $(i=1,3)$, and $a^+(\vec{k}_1)$ and $b^+(\vec{k}_3)$ are creation operators for the constituents that act on the vacuum state $|0\rangle$. The state is "covariantly" normalized in the volume V, so that

$$\langle B_1,\vec{p}_B=0,R|B_1,\vec{p}_B=0,S\rangle=2m_{B_1}V\delta_{RS}$$

$$\text{if}\int\frac{d^3k_1}{(2\pi)^3}|\psi_1(\vec{k}_1)|^2=1\ . \tag{10}$$

The matrix element for the decay $(\pi^+e^-)\to(\mu^+e^-)+\nu_\mu$ is then written as[1]

$$M_{rs}=\frac{4G_FV_{ud}}{\sqrt{2}}\sqrt{4m_{B_1}m_{B_2}}\times\int\frac{d^3k_1}{(2\pi)^3}\frac{\psi_1(\vec{k}_1)}{\sqrt{2k_1^0}}\frac{\psi_2^*(\vec{k}_2)}{\sqrt{2k_2^0}}S_{rs}\frac{f_\pi m_\pi}{2}\ , \tag{11}$$

$$S_{rs}=\bar{u}_r(\vec{q})\gamma_0\frac{1-\gamma_5}{2}v_s(\vec{k}_1-\vec{q})\ ,$$
$$k_2^0=[m_\mu^2+(\vec{k}_1-\vec{q})^2]^{1/2}\ , \tag{12}$$

where $f_\pi\approx 130$ MeV is the pion decay constant, and V_{ud} is the relevant Cabibbo-Kobayashi-Maskawa (CKM) matrix element. Here $u_r(\vec{q})$ and $v_s(\vec{k}_1-\vec{q})$ are the Dirac spinors of, respectively, the neutrino with spin r and the muon with spin s. The argument $\vec{k}_2$ of the bound state wave function ψ_2^* is given by $\vec{k}_2=\vec{k}_1-(m_{\text{red},2}/m_\mu)\vec{q}$. Note that in S_{rs} we have kept only the zeroth component of the weak current since the pion is essentially at rest. In the limit $\vec{k}_1-\vec{q}\ll m_\mu$, only the large components of the spinor need to be retained, and S_{rs} takes the simple form

$$S_{rs}=\frac{1}{2}\sqrt{2m_\mu|\vec{q}|}\left[\chi_r^+\left(1-\frac{\vec{\sigma}\cdot\vec{q}}{|\vec{q}|}\right)\varepsilon\chi_s\right]\ ,$$
$$\varepsilon=i\sigma_2,\quad\chi_1^+=(1,0),\quad\chi_2^+=(0,1)\ . \tag{13}$$

We square the matrix element, sum over pseudoscalar and vector final states, and average over the spin of the initial state. Using

$$\sum_{rs}S_{rs}S_{rs}^*=2m_\mu|\vec{q}|\ , \tag{14}$$

the spin-averaged matrix element becomes

$$\overline{|M|^2_\Sigma}=4G_F^2|V_{ud}|^2f_\pi^2m_\pi^2|F(\vec{q}^2)|^2m_\mu|\vec{q}|\ ,$$
$$F(\vec{q}^2)=\int\frac{d^3k_1}{(2\pi)^3}\psi_1(\vec{k}_1)\psi_2^*(\vec{k}_2)\ , \tag{15}$$

where we have used [see Eq. (11)] the approximation $4k_1^0k_2^0\approx 4m_{B_1}m_{B_2}$. The two-body kinematics fixes the momentum transfer $|\vec{q}|$ to be

$$|\vec{q}|=(m_{B_1}^2-m_{B_2}^2)/(2m_{B_1})\approx(m_\pi^2-m_\mu^2)/(2m_\pi)\ . \tag{16}$$

The decay rate in this approximation is

$$\Gamma=\frac{m_\pi^2-m_\mu^2}{16\pi m_\pi^3}\overline{|M|^2_\Sigma}\ . \tag{17}$$

To get an estimate of the errors made by using nonrelativistic mechanics, we calculated the decay rate of a free pion making the same approximations, i.e., just taking the zeroth component of the weak current and retaining only the large components of the Dirac spinor of the muon. We find

$$\Gamma_{\text{free}}^{\text{approx}}=\frac{G_F^2|V_{ud}|^2f_\pi^2m_\pi m_\mu(m_\pi^2-m_\mu^2)^2}{8\pi m_\pi^3}\ . \tag{18}$$

This differs from the rate calculated using relativistic mechanics only by the factor

$$\Gamma_{\text{free}}^{\text{exact}}/\Gamma_{\text{free}}^{\text{approx}}=m_\pi/m_\mu\approx 1.3\ , \tag{19}$$

which indicates a possible error of about 30%. The branching ratio for decay to the $1S$ state, obtained by dividing Eq. (17) by the approximate form in Eq. (18), is

$$B\frac{(\pi^+\mu^-)\to(\mu^+e^-)\nu_\mu}{\pi^+\to\mu^+\nu_\mu}=|F(\vec{q}^2)|^2\ . \tag{20}$$

Using the Schrödinger wave functions of Eq. (5) (with $Z=1$ of course) this is 4.51×10^{-11}.

III. RELATIVISTIC EFFECTS IN MUONIC TO ELECTRONIC ATOM DECAYS

We now consider the transition $(\mu^-Z)\to(e^-Z)\nu_\mu\bar{\nu}_e$, using with obvious replacements the same kinematics as in Fig. 1. This is a close analogue to the hadronic decay $B\to De\nu$. For simplicity we will take the nucleus to be spinless. As we now consider a three-body decay, we first discuss the range of the relevant kinematical variables. Because the two constituents have extremely different masses (especially if Z is large), it is useful to write the masses m_{B_1} and m_{B_2} of the bound states B_1 and B_2 in the form

[1] We use spinors normalized as $\bar{u}_r(\vec{p})u_s(\vec{p})=-\bar{v}_r(\vec{p})v_s(\vec{p})=2m\delta_{rs}$.

$$m_{B_1} = M + m_1, \quad \text{where } m_1 = m_\mu - E_{\text{bind},1} ,$$
$$m_{B_2} = M + m_2, \quad \text{where } m_2 = m_e - E_{\text{bind},2} . \qquad (21)$$

Here M is the mass of the heavy nucleus. In the rest frame of the decaying atom, the momentum transfer $|\vec{q}|$ to the neutrino pair is kinematically restricted to the range

$$0 \le |\vec{q}| \le (m_{B_1}^2 - m_{B_2}^2)/(2m_{B_1}) = (m_1 - m_2) + O(1/M) . \qquad (22)$$

For a given value of $|\vec{q}|$, the fourth component q^0 as seen in the rest frame and the square of the four-vector , q^2, are fixed:

$$q^0 = (m_1 - m_2) + O(1/M), \quad q^2 = (m_1 - m_2)^2 - \vec{q}^2 . \qquad (23)$$

Thus q^2 lies in the range $[0, (m_1 - m_2)^2]$. The momentum transfer $|\vec{q}|$ is always very small compared to the masses of the bound states, so the bound states can be considered to be at relative rest; in this approximation our formalism will still be covariant up to $O(1/M)$ corrections. Writing the relevant four-Fermi operator for muon decay in charge retention form, the matrix element for the transition reads

$$M_{sr} = \frac{4G_F}{\sqrt{2}} \sqrt{4m_{B_1} m_{B_2}} N_\mu S^\mu_{sr} , \qquad (24)$$

where

$$N_\mu = \bar{u}(p_{\nu_\mu}) \gamma_\mu \frac{1-\gamma_5}{2} v(p_{\nu_e}) , \qquad (25)$$

$$S^\mu_{sr} = \int \frac{d^3k_1}{(2\pi)^3} \psi_1(\vec{k}_1) \psi_2^*(\vec{k}_1 - \vec{q}) \frac{\bar{u}_s(e; \vec{k}_1 - \vec{q})}{\sqrt{2k_2^0}} \times \gamma^\mu \frac{1-\gamma_5}{2} \frac{u_r(\mu; \vec{k}_1)}{\sqrt{2k_1^0}} , \qquad (26)$$

$$k_1^0 = \sqrt{m_\mu^2 + \vec{k}_1^2}, \quad k_2^0 = \sqrt{m_e^2 + (\vec{k}_1 - \vec{q})^2} . \qquad (27)$$

The muon spin r and the electron spin s are just the spins of the bound states B_1 and B_2. In general a Wigner rotation [4] must be used to relate spins in two different frames, but here the rotation is essentially unity because the velocity of B_2 relative to B_1 is small.

We seek an expression for M_{sr} that is correct to zeroth order in $1/M$. This is found most easily by first writing the trivial identity

$$S^\mu_{sr} = \delta_{ss'} S^\mu_{s'r'} \delta_{r'r} , \qquad (28)$$

and then by rewriting the Kronecker δ's in terms of the spinors for the bound states and their constituents:

$$\delta_{r'r} = [2m_{B_1}(k_1^0 + m_\mu)]^{-1/2} \bar{u}_{r'}(\mu; \vec{k}_1) u_r(B_1; \vec{0}) ,$$
$$\delta_{ss'} = [2m_{B_2}(k_2^0 + m_e)]^{-1/2} \bar{u}_s(B_2; \vec{p}_{B_2}) u_{s'}(e; \vec{k}_1 - \vec{q}) . \qquad (29)$$

The first relation is exact, and the second introduces errors only $O(1/M)$. Then S^μ_{sr} can be written as

$$S^\mu_{sr} = (4m_{B_1} m_{B_2})^{-1/2} \bar{u}_s(B_2; \vec{p}_{B_2}) T^\mu u_r(B_1; \vec{0}) , \qquad (30)$$

where T^μ may be derived using Eqs. (26), (28), and (29). By repeatedly using the Dirac equations

$$\gamma^0 u_r(B_1; \vec{0}) = u_r(B_1; \vec{0}) ,$$
$$\bar{u}_s(B_2; \vec{p}_{B_2}) \gamma^0 = \bar{u}_s(B_2; \vec{p}_{B_2}) + O(1/M) , \qquad (31)$$

and dropping terms $\sim q^\mu$, which vanish when contracting with the neutrino tensor N_μ of Eq. (25), we arrive after some not completely straightforward algebra at

$$T^\mu = F_1(q^2)\gamma^\mu L + F_2(q^2)\gamma^\mu R + F_3(q^2)\gamma^\mu \frac{\not{q}}{m_\mu} L + F_4(q^2)\gamma^\mu \frac{\not{q}}{m_\mu} R . \qquad (32)$$

Here $L = (1-\gamma_5)/2$, and $R = (1+\gamma_5)/2$, and the form factors $F_i(q^2)$ are given as

$$F_i(q^2) = \int \frac{d^3k_1}{(2\pi)^3} \psi_1(\vec{k}_1) \psi_2^*(\vec{k}_1 - \vec{q}) \times \frac{h_i}{\sqrt{4k_1^0 k_2^0 (k_1^0 + m_\mu)(k_2^0 + m_e)}} , \qquad (33)$$

with

$$h_1 = (k_1^0 + m_\mu)(k_2^0 + m_e) + q^0[(1-C)(k_1^0 + m_\mu) - C(k_2^0 + m_e)] + (B - C)(q^0)^2 - A ,$$
$$h_2 = (C - B)q^2 - 2A ,$$
$$h_3 = [(1-C)(k_1^0 + m_\mu) + (B - C)q^0] m_\mu ,$$
$$h_4 = [C(k_2^0 + m_e) - (B - C)q^0] m_\mu . \qquad (34)$$

The quantities A, B, and C are

$$A = \frac{\vec{q}^2 \vec{k}_1^2 - (\vec{k}_1 \cdot \vec{q})^2}{2\vec{q}^2}, \quad B = \frac{3(\vec{k}_1 \cdot \vec{q})^2 - \vec{q}^2 \vec{k}_1^2}{2(\vec{q}^2)^2} ,$$
$$C = \frac{\vec{k}_1 \cdot \vec{q}}{\vec{q}^2} . \qquad (35)$$

The form factors F_i may seem noncovariant, because after the integration $d^3\vec{k}_1$ the variables q^0 and $|\vec{q}|$ remain as well as the square of the four-momentum q^2. But the form factors were derived in the rest frame of B_1, so q^0 and $|\vec{q}|$ are functions only of q^2 according to Eq. (23).

In terms of the quantities introduced, the matrix element can be written in the suggestive form

$$M_{sr} = \frac{4G_F}{\sqrt{2}} \bar{u}(p_{\nu_\mu}) \gamma_\mu L v(p_{\nu_e}) \bar{u}_s(B_2; \vec{p}_{B_2}) T^\mu u_r(B_1; \vec{0}) . \qquad (36)$$

The calculation of the decay rate, differential in the momentum transfer $|\vec{q}|$, is now standard. Expressing the bound state masses m_{B_1} and m_{B_2} in terms of M, m_1, and m_2 as defined in Eq. (21), one obtains

$$\frac{d\Gamma}{d|\vec{q}|} = \frac{G_F^2|\vec{q}|^2}{12\pi^3} K(|\vec{q}|) ,$$

$$K(|\vec{q}|) = [q^2 + 2(m_1 - m_2)^2](F_1^2 + F_2^2) + \frac{q^2}{m_\mu^2}[4(m_1 - m_2)^2 - q^2](F_3^2 + F_4^2)$$
$$-6q^2 \left[F_1F_2 + \frac{q^2}{m_\mu^2}F_3F_4 + \frac{m_1 - m_2}{m_\mu}(F_1 - F_2)(F_3 - F_4)\right] , \quad (37)$$

where the F_i are the form factors defined in Eq. (33). Note that m_1 and m_2 enter only through their difference; this is clear from the decomposition (21), which is invariant under the change of variables $M \to M + \lambda$ and $m_i \to m_i - \lambda$.

The wave functions that enter the form factors F_i in Eq. (33) are plotted in Figs. 2 and 3 (solid line). For comparison we have also drawn the wave functions for a point nucleus. The finite size of the nucleus affects the muon $1S$ wave function at high Z, as shown in Fig. 2. The finite size also affects the ultrarelativistic momentum tail of the electron $1S$ wave function, as shown in Fig. 3. The calculation of these wave functions is discussed in detail in the Appendix. Briefly, we have approximated the shape of a nucleus of atomic number A as a homogeneously charged sphere of radius $r_0 = 1.3A^{1/3}$ fm. In position space we solve the Dirac equation inside and outside r_0; the condition that these solutions match at $r = r_0$ determines the ground state wave function. We then take its Fourier transform.

From the kinematics [see Eq. (22)] it is clear that the muon $1S$ wave function is tested to momenta the order of m_μ. As shown in Fig. 2, relativistic effects are moderate. However, the finite size of the nucleus enhances the low momentum part of the muon wave function, which is fortunate because for lower momenta the electron wave function is large, and so the overlap increases. The electron $1S$ wave function is also tested up to momenta the order of m_μ and so the ultrarelativistic tail of the Dirac wave function is important. As shown in Fig. 3 the finite size of the nucleus diminishes the tail, and so the overlap with muon wave function decreases. For a nucleus with $Z \approx 80$, we find that the two effects associated with the finite size of the nucleus balance remarkably, giving approximately the same branching ratio (defined below), as the calculation using a point nucleus.

Using the same approximations, we also calculate the free-electron decay rate $\Gamma_{e,\text{free}}$ for $(Z\mu^-)$ decays. We write the mass of the bound state B_1 as $m_{B_1} = M + \hat{\gamma}m_\mu$, so that $\hat{\gamma}m_\mu$ is the total energy of the muon [see Eq. (22)]. We find

$$\Gamma_{e,\text{free}} = \Gamma^0\hat{\gamma}^2\langle L^{-1}\rangle ,$$
$$\langle L^{-1}\rangle = \int \frac{d^3k_1}{(2\pi)^3}|\psi_1(\vec{k}_1)|^2 \frac{m_\mu}{\sqrt{k_1^2 + m_\mu^2}} , \quad (38)$$

where $\Gamma^0 = G_F^2 m_\mu^5/(192\pi^3)$ is the decay width of a free muon, and $\langle L^{-1}\rangle$ can be interpreted as the mean inverse Lorentz factor representing the slowing of the muon decay rate due to its orbital velocity. Numerically, we have $\langle L^{-1}\rangle = 0.96$, for $Z = 80$ and $A = 200$; and $\langle L^{-1}\rangle = 1.00$, for $Z = 10$ and $A \leq 20$. For $Z = 80$ and $A = 200$, numerically $\hat{\gamma}$ is 0.91; for a point nucleus with $Z = 80$ note that $\hat{\gamma}$ and $\langle L^{-1}\rangle$ are significantly smaller, $\hat{\gamma}\,[1 - (Z\alpha)^2]^{1/2} = 0.81$ and $\langle L^{-1}\rangle = 0.85$. The branching ratio for the decay of a bound muon to produce a $1S$, instead of a free, electron in the final state is obtained by numerically integrating the spectrum in Eq. (37) and then by dividing by $\Gamma_{e,\text{free}}$ as given by Eq. (38). Using Dirac wave functions, the results for $Z = 80$ are

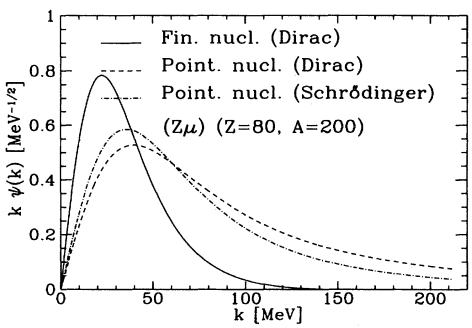

FIG. 2. Schrödinger and Dirac wave functions (multiplied by $|\vec{k}|$) for a $(Z\mu^-)$ atom with $Z = 80$.

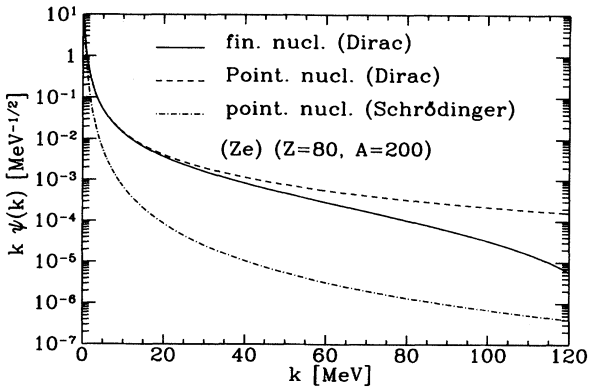

FIG. 3. Schrödinger and Dirac wave functions (multiplied by $|\vec{k}|$) for a (Ze^-) atom with $Z = 80$.

$$B\frac{(Z\mu^-) \to (Ze^-)\nu_\mu\bar{\nu}_e}{(Z\mu^-) \to Ze^-\nu_\mu\bar{\nu}_e} = \begin{cases} 3.59 \times 10^{-5} & \text{(finite nucleus, } A = 200) \text{ ,} \\ 3.60 \times 10^{-5} & \text{(point nucleus) .} \end{cases} \tag{39}$$

We note that the finite size of the nucleus leaves the branching ratio essentially unchanged. The effect of the finite size will be even smaller for smaller Z, so we can calculate the branching ratio for $Z = 10$ using the Dirac wave functions for a point nucleus. We get

$$B\frac{(Z\mu^-) \to (Ze^-)\nu_\mu\bar{\nu}_e}{(Z\mu^-) \to Ze^-\nu_\mu\bar{\nu}_e} = 2.48 \times 10^{-9}$$

$$\text{(point nucleus, } Z = 10) \text{ .} \tag{40}$$

To demonstrate the increase in the branching ratio due to the Dirac wave functions, we also show the branching ratio calculated using the Schrödinger wave functions for a point nucleus:

$$B\frac{(Z\mu^-) \to (Ze^-)\nu_\mu\bar{\nu}_e}{(Z\mu^-) \to Ze^-\nu_\mu\bar{\nu}_e} = \begin{cases} 6.98 \times 10^{-7} \ (Z = 80) \text{ ,} \\ 1.85 \times 10^{-9} \ (Z = 10) \text{ .} \end{cases} \tag{41}$$

The relativistic enhancement for $Z = 80$ is a remarkable factor of 50.

In Fig. 4 the decay distribution $d\Gamma/d|\vec{q}|$, normalized to unit integral, is given for $Z = 80$. For illustration we also give the spectra predicted using the Schrödinger and Dirac wave functions for a point nucleus. Comparing the latter two curves shows that relativistic effects cause the spectrum to peak at higher momenta. However, the finite nuclear size causes the shape of the spectrum to narrow again. This can easily be understood by looking at the muonic wave function in Fig. 2. In Fig. 5 the same distribution is shown for $Z = 10$; as might be expected both relativistic effects and the effect of a finite nuclear size are small. Transitions of the form $(Z\mu) \to (Ze) + \nu\bar{\nu}$ have as their signature a bound state recoiling with a large momentum the order of m_μ. The momentum distribution for heavy atoms ($Z = 80$) peaks at about 20 MeV as seen in Fig. 4.

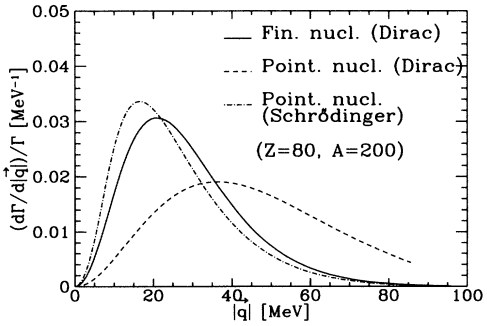

FIG. 4. Decay spectrum $d\Gamma/d|\vec{q}|$, normalized such that $\int d\Gamma/d|\vec{q}|d|\vec{q}| = 1$, for $Z = 80$. The solid line is obtained by using Dirac wave functions which take into account the finite size of the nucleus. The dashed (dashed-dotted) line corresponds to pointlike Dirac (Schrödinger) wave functions.

IV. PROSPECTS FOR EXPERIMENTAL TESTS

Prospects for an experimental test of atomic alchemy are very dim but not hopeless. While the branching ratio is too small to detect (π^+e^-) atoms, it may be detectable for muonic atoms. To see it one must prepare a sample of $(Z\mu^-)$ atoms with no electrons in the $1S$ state, and prevent electrons from refilling the $1S$ state over the ~ 1 μs lifetime of the muon. The increase in the calculated branching ratio with Z [see Eqs. (39) and (40)] would argue for high-Z experiment; however, as Z increases, the atomic nucleus no longer remains a passive spectator but absorbs muons at an increasing rate. Using the measured rates of Ref. [5], for neon and lead, we find the branching ratios with respect to the total rate at which $1S$ muons disappear are

$$B\frac{(Z\mu^-) \to (Ze^-)\nu_\mu\bar{\nu}_e}{(Z\mu^-) \to X} = \begin{cases} 1.70 \times 10^{-9} \ (Z = 10) \text{ ,} \\ 9.70 \times 10^{-7} \ (Z = 80) \text{ .} \end{cases} \tag{42}$$

Despite the increased capture rate, the increase in the yield per $1S$ muon near lead ($Z = 82$) remains a factor of 570 due to the large relativistic enhancement. Nevertheless, we shall examine a possible experiment using neon gas, instead of, say, xenon, because the most is known theoretically and experimentally about the lighter gas, and because the same difficulties, although of a different scale, are present in both.

On paper, the conditions for observing atomic alchemy in neon can be realized by injecting and capturing ~ 5 keV muons in a cyclotron trap [6] containing neon gas at a pressure of ~ 10 Pa. Muons of this energy injected into the trap's magnetic field will lose energy as they orbit and will come to rest in ~ 1 μs (adopting estimates in [6]) and be captured by a neon atom. The muons cascade rapidly to the $1S$ state, ejecting almost all of the atomic electrons. In neon the mean number of electrons remaining in the K shell has been measured [7] to be between 0.07 and 0.68 (to be compared with 2) by the time the

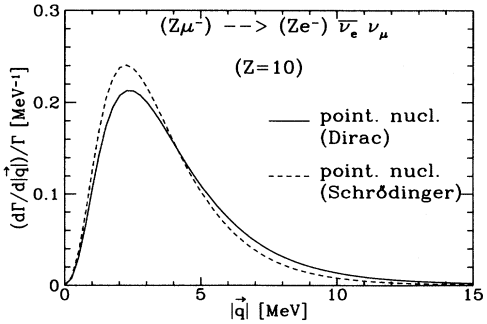

FIG. 5. Decay spectrum $d\Gamma/d|\vec{q}|$, normalized such that $\int d\Gamma/d|\vec{q}|d|\vec{q}| = 1$, for $Z = 10$. The solid (dashed) line corresponds to pointlike Dirac (Schrödinger) wave functions.

muon has fallen to states with principal quantum number $n = 5$, in agreement with simple estimates [8] of 0.25; the number remaining will diminish somewhat more as the muon continues to the $1S$ state. Total ionization of an atom has been observed in the cascades of antiprotons in atoms as heavy as krypton [9]; total ionization of neon by muons is however less probable because of the lighter muon mass and its weak binding energy. Nevertheless, in neon the electron K shell will often be vacant to receive the electron from the muon decay. At the low pressure of 10 Pa, the time taken for the ion $(\mathrm{Ne}\mu)^{9+}$ to capture an electron is also ~ 1 μs (using estimates [8] for the velocity of the ion, $\sim 10^5$ cm/s, and for the cross section for electron capture of Ne^{9+} on Ne, $\sim 3 \times 10^{-15}$ cm^2). Most of the captured muons will decay before the electron K shell can refill and block desired decay; furthermore, only 31% of the muons in the $1S$ state will be lost to muon capture [10].

Such a scheme involves scaling existing cyclotron traps from operating pressures [7] ~ 5000 Pa down to ~ 1 Pa. An application of Liouville's theorem shows that the radial and axial distribution of the particles in space when they come to rest is determined only by their radial and axial spread where they enter the trap, provided only that the rate at which the particles slow is small compared to the orbit frequency in the trap [6]. Once the particles are in the trap, lowering the gas pressure increases only the time it takes for them to come to rest. However, existing schemes for injecting particles into the trap rely on choosing the particles initial orbit to miss a moderator for the first few critical loops after they pass through it; after that they have slowed too much in the target gas ever to hit it again. Despite this difficulty, cyclotron traps have captured antiprotons when operated at gas pressures well below 10 Pa [6]. Such a scheme is much harder to work with injected muons, instead of antiprotons, because the muons being unstable cannot be stacked and cooled and so the emittance of the injected beam is much larger. Whether muons can be successfully injected in such a low-pressure trap at a rate as high as 10^7 s^{-1}, a rate which the high-pressure traps are expected to achieve [7], is a technical problem beyond the scope of this paper.

To see the alchemy transitions, once made to occur, is also difficult. The signature for the transition is the appearance of $^{20}\mathrm{Ne}^{9+}$ ions with a distribution dN/dq^2 extending to momenta the order of m_μ. These ions are difficult to distinguish from $^{20}\mathrm{F}^{9+}$ ions, made also with a momentum of m_μ by interval conversion. Nor will it be easy to extract any ions for analysis, because in neon at a pressure of 10 Pa a bare ion can fly only ~ 1 mm before capturing an electron, and the gas pressure cannot be lowered much without letting the muons in the trap decay in flight before they can be captured.

We have examined so far only the decay of a bare $(Z\mu)$ ion to a bound state. It is easy to estimate the decay rate when the electronic $1S$ state of the ion remains partly or wholly filled, either because electrons are captured from nearby atoms before the muon decays, or because (at high Z) the cascading muon fails to eject all the atomic electrons. When there is one electron in the K shell the rate is halved. When the K shell is full the electron from the muon decay will populate the L shell; we expect the rate for decay to a vacant L shell to be $\sim 1/8$ of the rate for decay to a vacant K shell, based on naive $1/n^3$ scaling. This estimate assumes that the only role of the K electrons is to Pauli-block the $1S$ state, and this is approximately true. For the probability that one electron in the $1S$ jumps to any other state when the nuclear charge changes from an effective charge of $Z-1$ to Z is, in the sudden approximation,

$$1 - \frac{Z^3(Z-1)^3}{(Z-\frac{1}{2})^6} \approx \frac{3}{4Z^2} \approx 0.008 \text{ in Ne} ,$$

and the probability that it jumps when a nucleus of charge Z acquires a recoil velocity v is [16]

$$1 - \left[1 + \left(\frac{v}{Z\alpha c}\right)\right]^{-4} \approx \left(\frac{2v}{Z\alpha c}\right)^2 ,$$

which is only 0.024 at the maximum recoil velocity of a neon nucleus and is certainly negligible when averaged over the velocity spectrum. In principle, promoting one of the original $1S$ electrons to the $2S$, to free the $1S$ state to receive an electron from the muon decay, is a path with an amplitude that interferes with that for the muon to decay directly to the $2S$; in practice, however, the effect is negligible.

V. CONCLUSIONS

We have calculated relativistically corrected rates for some weak transitions between electromagnetic bound states. For $(Z\mu)$ atoms and for large Z, the rate of these transitions and also the shapes of the spectra depend drastically on relativistic corrections; these corrections enhance the rate by a factor of 50 for $Z = 80$. The QED analysis of these alchemy transitions illustrates some of the physics of the relativistic wave functions that must invariably enter the QCD analysis of the corresponding exclusive electroweak decays of hadrons.

An experimental measurement of atomic alchemy, while conceivable for the favorable transition $(Z\mu^-) \to (Ze^-)\nu_\mu\bar{\nu}_e$, seems a remote prospect.

ACKNOWLEDGMENTS

We would like to thank P. Truöl, R. Engfer, I. B. Khriplovich, and M. Strikman for stimulating discussions. This work was partially supported by Schweizerischer Nationalfonds and the Department of Energy under Contract No. DE-AC03-76SF00515.

APPENDIX: DIRAC WAVE FUNCTIONS

In atomic alchemy $(Z\mu) \to (Ze)\nu_\mu\bar{\nu}_\mu$ the electron wave function is probed at momenta the order of m_μ.

Schrödinger wave functions are not appropriate and the Dirac wave functions [11] must be used. Recoil corrections due to the finite nuclear mass are extremely small, so the Dirac wave functions for an electron in the field of an infinitely heavy nucleus will describe adequately the high momentum tail of the electron (and muon) wave function. At large Z the Bohr radius of the muon $1S$ state is less than the nuclear radius, so the effect of the finite size of the nucleus on the muon wave function must obviously be included; the effect of the finite size is also important on the high-momentum tail of the electron $1S$ wave function.

We sketch how the momentum-space wave functions $\psi_1(\vec{k})$ and $\psi_2(\vec{k})$ that appear in the form factors in Eq. (33) are extracted from the usual four-component Dirac wave functions in position space. Because everything can be worked out analytically for a point nucleus, we describe this case first.

1. Point nucleus

From the literature (e.g., from [11] on p. 55) we take the (four-component) ground state wave function in position space, $\psi_{n=1,j=1/2,j_z=1/2}(r,\theta,\phi)$. For brevity we write this as $\Phi(\vec{x})$. Taking the Fourier transform, we get the wave function in momentum space:

$$\tilde{\Phi}(\vec{k}) = \int d^3x \Phi(\vec{x}) \exp(-i\vec{k}\cdot\vec{x}) \ , \tag{A1}$$

$$\tilde{\Phi}(\vec{k}) = \begin{pmatrix} \hat{f}(k) \begin{pmatrix} 1 \\ 0 \end{pmatrix} \\ \\ \hat{g}(k) \frac{\vec{\sigma}\cdot\vec{k}}{k} \begin{pmatrix} 1 \\ 0 \end{pmatrix} \end{pmatrix}, \quad k = |\vec{k}| \ , \tag{A2}$$

with

$$\hat{f}(k) = \frac{N}{k(1+a^2k^2)^{1+\gamma/2}} (\sin\rho + ak\cos\rho) \ , \tag{A3}$$

$$\hat{g}(k) = \frac{Nm(1-\gamma)}{\gamma k^2 (1+a^2k^2)^{1+\gamma/2}} \{[1+(1+\gamma)a^2k^2]\sin\rho - \gamma ak\cos\rho\} \ , \tag{A4}$$

$$a = \frac{1}{mZ\alpha}, \quad \gamma = \sqrt{1-(Z\alpha)^2}, \quad \rho = \gamma \arctan(ak), \quad N = 2^{\gamma+1}\Gamma(1+\gamma)\sqrt{\frac{a\pi(1+\gamma)}{\Gamma(1+2\gamma)}} \ . \tag{A5}$$

Here m denotes the reduced mass of the system, which we take to be identical to that of the muon or the electron because we work to lowest order in $1/M$. The corresponding energy eigenvalue is then $E = m\gamma$. For $Z = 80$ the numerical value of γ is 0.81.

The Dirac wave function for a bound state of course projects onto plane waves of both positive and negative energies; the latter waves correspond to antiparticles. We therefore define the relevant wave function (to be used in calculating the form factors) by the projection on positive energy plane waves. Thus we expand $\tilde{\Phi}(\vec{k})$ in terms of spinors $u_r(\vec{k})$ and $v_r(-\vec{k})$, writing

$$\tilde{\Phi}(\vec{k}) = \sum_r \left[A_r(\vec{k}) \frac{u_r(\vec{k})}{\sqrt{2k^0}} + B_r^*(-\vec{k}) \frac{v_r(-\vec{k})}{\sqrt{2k^0}} \right] \ ,$$

$$k^0 = \sqrt{\vec{k}^2 + m^2} \ . \tag{A6}$$

If $j_z = 1/2$ we get

$$A_{+1/2}(\vec{k}) = \sqrt{\frac{k^0+m}{2k^0}} \left(\hat{f}(k) + \frac{k}{k^0+m}\hat{g}(k) \right),$$

$$A_{-1/2} = 0 \ , \tag{A7}$$

$$B^*_{+1/2}(-\vec{k}) = -\sqrt{\frac{k^0+m}{2k^0}} \frac{(k^1+ik^2)}{k} \times \left(\frac{k}{k^0+m}\hat{f}(k) - \hat{g}(k) \right) \ ,$$

$$B^*_{-1/2}(-\vec{k}) = \sqrt{\frac{k^0+m}{2k^0}} \frac{k^3}{k} \left(\frac{k}{k^0+m}\hat{f}(k) - \hat{g}(k) \right) \ .$$

Here $A_r(\vec{k})$ is the probability amplitude to find an electron with momentum $\vec{k}$ and spin r in the atom, while $B_r^*(-\vec{k})$ is the probability amplitude to find a positron with momentum $\vec{k}$ and spin r; the latter amplitude arises from the creation of e^+e^- pairs on the nucleus. Because the wave function in position space is normalized as $\int d^3x \Phi^+(\vec{x})\Phi(\vec{x}) = 1$, the Fourier transform is automatically normalized as $\int [d^3k/(2\pi)^3] \tilde{\Phi}^+(\vec{k})\tilde{\Phi}(\vec{k}) = 1$. Therefore $A_r(\vec{k})$ and $B_r^*(-\vec{k})$ are normalized so that

$$\int \frac{d^3k}{(2\pi)^3} \sum_r \{|A_r(\vec{k})|^2 + |B_r(\vec{k})|^2\} = 1 \ . \tag{A8}$$

The integral $\int [d^3k/(2\pi)^3] \sum_r |B_r(\vec{k})|^2$ gives the probability to find a three particle Fock state $(e^+e^-e^-)$ in the atom. Even for $Z = 80$ this fraction is tiny ($\approx 0.2\%$), so we only consider the one-Fock contribution characterized by $A_r(\vec{k})$. We mention that if we consider the atom with $j_z = -\frac{1}{2}$, we get $A_{+1/2}(\vec{k}) = 0$, and $A_{-1/2}(\vec{k})$ is identical to $A_{+1/2}(\vec{k})$, given in Eq. (A7) for $j_z = +\frac{1}{2}$. The wave function denoted in the text as $\psi(\vec{k})$ is therefore given in the relativistic case by

$$\psi(\vec{k}) = A_{+1/2}(\vec{k}) \ . \tag{A9}$$

Because the coefficients B_r are very small, the effects of antiparticle production are small, and we get essentially

the same form factor as we would have gotten had we naively computed the simple overlap of the wave functions in position space.

2. Finite-size nucleus

As usual (see, e.g., [12]), we model a nucleus of atomic number A as a homogeneously charged sphere of radius $r_0 = 1.3A^{1/3}$ fm; numerically $r_0 \approx 7$ fm for $A = 200$. Inside the sphere the potential has the form $V(r) = -(Z\alpha/r_0)(3 - r^2/r_0^2)/2$, and outside we have $V(r) = -Z\alpha/r$. In the notation of Landau-Lifschitz [13] we write the four-component Dirac function $\Phi(\vec{r})$ as

$$\Phi(\vec{r}) = N \begin{pmatrix} f(r)\begin{pmatrix}1\\0\end{pmatrix} \\ -ig(r)\frac{\vec{\sigma}\cdot\vec{r}}{r}\begin{pmatrix}1\\0\end{pmatrix} \end{pmatrix}, \quad r = |\vec{r}| , \tag{A10}$$

where the constant N is chosen such that $\int d^3r\Phi^+(\vec{r})\Phi(\vec{r}) = 1$. The radial equations for f and g are

$$f'(r) - [E + m - V(r)]g(r) = 0 ,$$
$$g'(r) + \frac{2}{r}g(r) + [E - m - V(r)]f(r) = 0 , \tag{A11}$$

which are solved separately in the two regions $r \le r_0$ and $r \ge r_0$ for an arbitrary constant $E < m$. In the outer region $r \ge r_0$ there is (up to an overall constant) exactly one solution (f, g) that is square integrable at $r = \infty$. It is given by (see Landau and Lifschitz [13])

$$f(r) = \sqrt{m+E}\exp(-\lambda r)r^{\gamma-1}(Q_1 + Q_2) ,$$
$$g(r) = -\sqrt{m-E}\exp(-\lambda r)r^{\lambda-1}(Q_1 - Q_2) ,$$
$$Q_1 = U\left(\gamma - \frac{Z\alpha E}{\lambda}, 2\gamma+1, 2\lambda r\right) ,$$
$$Q_2 = -\left(1 - \frac{Z\alpha m}{\lambda}\right)U\left(\gamma+1-\frac{Z\alpha E}{\lambda}, 2\gamma+1, 2\lambda r\right) ,$$
$$\lambda = \sqrt{m^2 - E^2}, \gamma = \sqrt{1-(Z\alpha)^2} . \tag{A12}$$

The hypergeometric function U is defined and discussed in detail in Chap. 13 of Ref. [14]; it is also related to Whitaker functions, which are numerically accessible in the CERN library.

In the inner region ($r \le r_0$) a simplified solution for the (massless) electron has been obtained by Khriplovich [15]; however, the substantial mass of the muon requires a more complete treatment. It turns out that the Dirac equation has (again up to an overall constant) exactly one solution (f, g) that is square integrable at $r = 0$; in the present case it has a Taylor series expansion around $r = 0$. While f starts as a constant, g begins with a term linear in r. The coefficients of the power series expansions of f and g may be defined recursively.

The inner and outer solutions must satisfy the matching condition

$$(f/g)_{r\to r_{0-}} = (f/g)_{r\to r_{0+}} \tag{A13}$$

in order to be solutions of the complete equation. This can only hold for certain values of E; these are just the eigenvalues. For $Z = 80$ and $A = 200$ the lowest eigenvalues for $E = 0.908m_\mu$ and $E = 0.811m_e$ for the $1S$ states of the muon and the electron, respectively.

The Fourier transform $\tilde{\Phi}(\vec{k})$ is then defined and written in terms of $\hat{f}(k)$ and $\hat{g}(k)$ precisely as in Eqs. (A1) and (A2). Proceeding through the same steps as for a point nucleus, one finally gets the wave function $\psi(\vec{k})$ [compare with Eq. (A9)] in a numerical form. This wave function is shown for the $(Z\mu)$ and the (Ze) atoms in Figs. 2 and 3, respectively.

[1] S. J. Brodsky and P. Lepage, Phys. Rev. D **22**, 2157 (1980).
[2] W. Caswell and P. Lepage, Phys. Rev. A **18**, 810 (1978).
[3] A. B. Migdal, in *Qualitative Methods in Quantum Theory*, edited by D. Pines, Frontiers in Physics series Vol. 48 (Benjamin, New York, 1977).
[4] C. Greub and D. Wyler, Phys. Lett. B **295**, 293 (1992).
[5] See C. Rubbia, in *High Energy Physics*, edited by E. H. S. Burhop (Academic, New York, 1969), Table VI.
[6] L. M. Simons, in *Fundamental Symmetries*, edited by P. Bloch (Plenum, New York, 1987), p. 89; see also [7].
[7] R. Bacher, P. Blüm, D. Gotta, K. Heitlinger, and M. Schneider, Phys. Rev. A **39**, 1610 (1989).
[8] R. Bacher, D. Gotta, L. M. Simons, J. Missimer, and N. M. Mukhopadhyay, Phys. Rev. Lett. **54**, 2087 (1985).
[9] R. Bacher, P. Blüm, D. Gotta, K. Heitlinger, M. Schneider, J. Missimer, L. M. Simons, and K. Elsener, Phys. Rev. A **38**, 4395 (1988).
[10] J. L. Rosen, E. W. Anderson, E. J. Bleser, L. M. Lederman, S. L. Meyer, J. E. Rothberg, and I. T. Wang, Phys. Rev. **132**, 2691 (1963).
[11] J. D. Bjorken and S. D. Drell, in *Relativistic Quantum Mechanics*, edited by L. I. Schiff, International Series in Pure and Applied Physics (McGraw-Hill Company, New York, 1964), Vol. 1.
[12] H. Behrends and W. Bühring, *Electron Radial Wave Functions and Nuclear Beta-Decay*, International Series of Monographs on Physics Vol. 67 (Clarendon, Oxford,

1982).
[13] L. D. Landau and E. M. Lifschitz, *Course of Theoretical Physics, Volume 4: Quantum Electrodynamics* (Pergamon Press, Oxford, 1982).
[14] M. Abramowitz and A. Stegun, *Handbook of Mathematical Functions* (Dover, New York, 1972).
[15] I. B. Khriplovich, *Parity Nonconservation in Atomic Phenomena* (Gordon and Breach, New York, 1991).
[16] J. D. Jackson, Phys. Rev. **106**, 330 (1957).